JOURNAL OF CHEMICAL INFORMATION AND MODELING

Article

pubs.acs.org/jcim

Transport Behavior of a Single Ca^{2+}, K^+, and Na^+ in a Water-Filled Transmembrane Cyclic Peptide Nanotube

Xiliang Yan, Jianfen Fan,* Yi Yu, Jian Xu, and Mingming Zhang

College of Chemistry, Chemical Engineering and Materials Science, Soochow University, Suzhou 215123, People's Republic of China

Supporting Information

ABSTRACT: Molecular dynamics simulations have been performed to investigate the transport properties of a single Ca^{2+}, K^+, and Na^+ in a water-filled transmembrane cyclic peptide nanotube (CPNT). Two transmembrane CPNTs, i.e., 8×$(WL)_{n=4,5}$/POPE (with uniform lengths but various radii), were applied to clarify the dependence of ionic transport properties on the channel radius. A huge energy barrier keeps Ca^{2+} out of the octa-CPNT, while Na^+ and K^+ can be trapped in two CPNTs. The dominant electrostatic interaction of a cation with water molecules leads to a high distribution of channel water around the cation and *D*-defects in the first and last gaps, and significantly reduces the axial diffusion of channel water. Water-bridged interactions were mostly found between the artificially introduced Ca^{2+} and the framework of the octa-CPNT, and direct coordinations with the tube wall mostly occur for K^+ in the octa-CPNT. A cation may drift rapidly or behave lazily in a CPNT. K^+ behaves most actively and can visit the whole deca-CPNT quickly. The first solvation shells of Ca^{2+} and Na^+ are basically saturated in two CPNTs, while the hydration of K^+ is incomplete in the octa-CPNT. The solvation structure of Ca^{2+} in the octa-CPNT is most stable, while that of K^+ in the deca-CPNT is most labile. Increasing the channel radius induces numerous interchange attempts between the first-shell water molecules of a cation and the ones in the outer region, especially for the K^+ system.

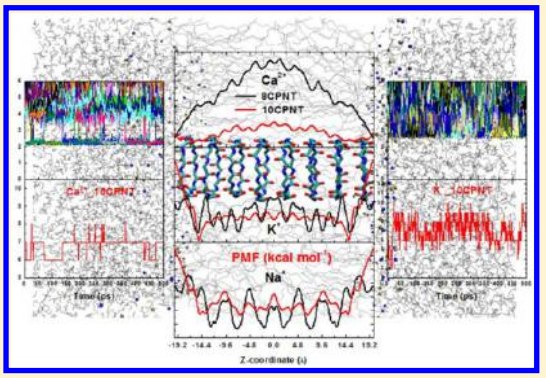

INTRODUCTION

In-depth studies on cyclic peptide nanotubes (CPNTs) started from the first CPNT of 8×cyclo-[(L-Gln-D-Ala-L-Glu-D-Ala)$_2$-] synthesized by Ghadiri et al. in 1993.[1] The open-ended, hollow, and tubular structure of a CPNT provides the possibility to conduct molecules and ions,[2−4] just like a natural biological channel.[5−7] Particularly, a CPNT with a hydrophobic outer surface, which can be easily embedded into a lipid bilayer, can serve as a good model imitating the biological function of a natural transmembrane channel.[8−10]

Previous researchers have succeeded in using the KcsA potassium channel[11−13]and NavAb sodium channel[14−16] as models for understanding the structure−function relationships of ion channels. Similar to carbon nanotubes (CNTs) once widely applied for ion transport,[17−21] CPNTs have been considered as fine artificial ion channels since 1994 by Ghadiri et al.,[22] who found the conductances of Na^+ and K^+ through a CPNT to be up to 3 times faster compared with the results in gramicidin A (GA). Using a steered molecular dynamics (SMD) simulation, Hwang et al.[23] executed a specific and elaborate investigation on ion transport by calculating the potential of mean force (PMF) of a single Na^+ or K^+ passing through a CPNT embedded in water, providing us a profound insight into the conductance difference between Na^+ and K^+. Their research brought about a fervor of probing deeply into ion transport through a CPNT. By designing a minimal CP subunit consisting of only four Gly residues, Sumiya et al.[24] assembled an aggregated form (a CPNT) with nine CP subunits and found that the CPNT backbone may be destroyed when an anion (F^-) passed through the channel. By calculating the PMF profiles of Na^+, K^+, and Cl^- permeating through a CPNT embedded in water on the basis of the umbrella sampling scheme and thermodynamic integration approach, respectively, Choi et al.[25] explored in detail the differences between the selectivities of the CPNT for a cation versus an anion, uncovering free energy wells for Na^+ and K^+ but barriers for Cl^- in the tube. Based on the PMF of Na^+ moving through an octa-CPNT, our previous work[26] revealed barriers for Na^+ in midplane regions and wells in α-plane zones. Granja et al.[27] studied the transport properties of several electrolyte solutions in self-assembled α,γ-peptide nanotubes and found that the assembled nanotubes were selective for alkaline ions. The distributions of radial density and dipole orientations of water molecules around Li^+, Na^+, or Rb^+ in a self-assembled cyclo-[(L-Ala-D-Ala)$_4$-] CPNT were found to be dependent on the location of the cation, i.e., in a midplane region or an α-plane zone.[28] The relative position of a channel mouth to a membrane surface is also responsible for the free energy delineating the translocation of an ion.[29] Electric field and temperature also have effects on the diffusions and hydrations of Na^+ and K^+ within a CPNT.[30,31] Compared with K^+ and

Received: January 16, 2015
Published: April 20, 2015

DOI: 10.1021/acs.jcim.5b00025
J. Chem. Inf. Model. 2015, 55, 998−1011

Na^+, there are hardly any investigations on the transport property of Ca^{2+} in a CPNT.

Ca^{2+}, K^+, and Na^+ are essential in numerous cellular processes. Ca^{2+} and Na^+ have similar ionic radii of ∼1.0 Å and are relatively smaller than K^+ (ionic radius: ∼1.5 Å). The existences of these cations in organisms are closely related to water environments. Detailed analysis of the ONIOM-XS (Our own N-layered Integrated molecular Orbital and molecular Mechanics-Exchange of Solvents) molecular dynamics (MD) trajectories gave 6.3 and 7.6 as the average hydration numbers for K^+ and Ca^{2+} in water, respectively.[32] High-level ab initio MD simulations determined the solvation structures of Na^+ and K^+ with 5.7−5.8 and 6.9−7.0 water molecules, respectively.[33] Corry et al.[21] observed a larger number (nearly 8) of water molecules in the first solvation shell of K^+ inside a (9,9) CNT than that in bulk (about 7). It was reported that the averaged residence time (τ_{Na^+} = 30 ps) of water molecules in the first hydration shell of Na^+ in a (12,12) CNT boron nitride nanotube was much larger than that (τ_{K^+} = 6 ps) in the K^+ system.[34] Lu et al.[19] found that the preferential orientations of water molecules in the coordination shells of Na^+ and K^+ in an infinitely long CNT at 298 K presented anomalous characteristics.

In this work, MD simulations were performed to investigate the transport properties of a single Ca^{2+}, K^+, and Na^+ in a water-filled transmembrane CPNT. Two transmembrane CPNTs with different channel radii, i.e., $8\times(W\underline{L})_{n=4,5}$/POPE, were used to investigate the dependences of the transport behaviors of a single Ca^{2+}, K^+, and Na^+ on channel radius, respectively, aiming to explore the comprehensive mechanisms underlying the interactions of these cations with a CPNT backbone and neighboring water, and revealing the solvation structures and the influences of these cations on the movement of channel water.

MATERIALS AND METHODS

System Preparations. To fully understand the dependences of the transport properties of Ca^{2+}, K^+, and Na^+ on channel radius, two CPNTs, i.e., $8\times(W\underline{L})_{n=4,5}$, wherein the underlined letter corresponds to a D-amino acid residual, were constructed. Each one has a uniform length of ∼33.6 Å, but different pore radius of ∼4.6 or 5.8 Å, composed of eight CP subunits divided into seven gaps, numbered sequentially along the major axis (*z*-axis) of the channel. The hydrophobic characteristics of the composed amino acid residues Trp (W) and Leu (L) guarantee that the two CPNTs can be easily embedded into a 1-palmitoyl-2-oleoyl-*sn*-glycero-3-phosphoethanolamine (POPE) membrane without a hitch. Two water boxes, each with a thickness of 26 Å, were added to two sides of a CPNT, respectively. A schematic diagram representing the system setup is shown in Figure 1. Each of two systems was equilibrated for 20 ns in a NPT ensemble with a periodic boundary condition at the temperature of 310 K and pressure of 1 bar, respectively. The specific approaches were similar to those in our former work.[35]

A single Ca^{2+}, K^+, or Na^+ was separately inserted at a position along a tube axis using Autoionize plugin of the molecular graphics program VMD 1.9.1.[36] Correspondingly, one or two Cl^- were randomly introduced in a water box to ensure the absolutely electrical neutrality of a simulation system. Six constructed systems, i.e., transmembrane octa- and deca-CPNTs with a single Ca^{2+}, K^+, and Na^+ in the channels, respectively, were further separately equilibrated for 10 ns with a time step of 1 fs in a NPT ensemble.

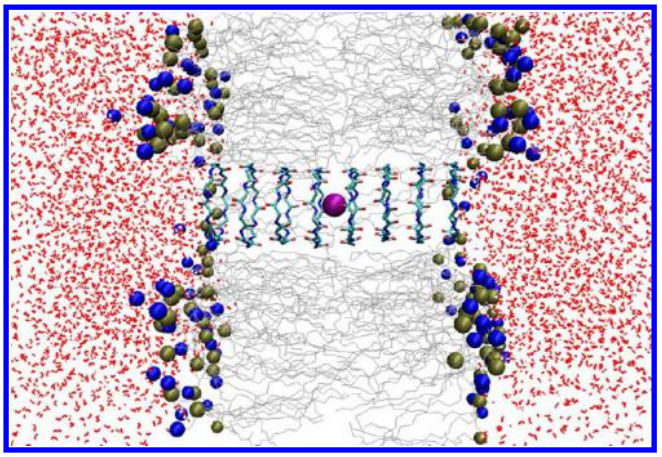

Figure 1. Snapshot of $8\times(W\underline{L})_5$-CPNT embedded in the fully hydrated POPE lipid bilayer, with a single K^+ implanted in the center of the channel. The N and P atoms of lipid units are represented in vdW spheres, and H atoms are ignored for clarity. The framework of the deca-CPNT is described in a stick style, K^+ in a vdW sphere. One Cl^- (not shown) was inserted in the side water box to neutralize the system. Other systems containing a single Ca^{2+}, K^+, and Na^+ in the octa- or deca-CPNTs are similar.

All the simulations were carried out using the program NAMD 2.9.[37] The simulation setup and trajectory analysis were performed using the graphics program VMD 1.9.1. The CHARMM27 force field[38] and TIP3P water model[39] were used to describe the CPNTs, POPE membrane, ions, and water molecules, respectively. The computation of full electrostatic interactions was carried out using the particle mesh Ewald method[40] with a periodic boundary condition. The Nosé−Hoover Langevin piston and Langevin dynamics methods[41] were applied to maintain the pressure and temperature of a system at 1 bar and 310 K, respectively. The spherical cutoff distance was uniformly selected as 12 Å for the computation of an electrostatic or van der Waals (vdW) force, with a switching function starting from 10 Å. To reduce the cost of computing nonbonded interactions, the parameter "pairlistdist" was applied to break off the search for pairs of atoms beyond 14 Å of atomic spacing. The SHAKE algorithm[42] was used to restrict the bond length between each hydrogen and its parent atom to an equilibrium value. To prevent a CPNT from drifting, a Harmonic potential of 10 kcal mol^{-1} $Å^{-2}$ was applied to each C_α atom of a CPNT during a MD simulation.

Potential of Mean Force. The PMF of a single cation along the tube axis (*z*-axis) of a CPNT was achieved by employing the adaptive biasing force (ABF) method[43,44] in its NAMD formulation and implementation. Prior to carrying out an ABF simulation, a constant velocity SMD (cv-SMD) simulation[23] was performed to gain a qualitative picture of the permeation pathway for a single cation moving through a CPNT. Here, a constant pulling speed of 2 Å/ns, which was fast enough for a cation to traverse a whole CPNT but not so quick to cause a measurement noise, was applied to a cation from its initial point (z = −20.0 Å, close to gap 1) to the destination at z = +20.0 Å (close to gap 7). To improve the efficiency of the ABF algorithm, the span of the reaction coordinate from −20 Å to +20 Å along the tube axis (*z*-axis) of a CPNT was divided into eight equally spaced windows. A PDB file of the entire system containing a cation in each window was

DOI: 10.1021/acs.jcim.5b00025
J. Chem. Inf. Model. 2015, 55, 998−1011

created from the above cv-SMD trajectory and used as the starting point for the following ABF simulation. A 10-ns ABF simulation for a cation in each window was carried out, long enough to ensure the convergence of the free energy calculation. In order to enhance the smoothness of a PMF profile, each window was further subdivided into 50 small bins with a width of 0.1 Å. To obtain a reasonable estimate of the force distribution, the first 1000 samples in each bin were discarded when applying the ABF sampling. The obtained outputs for a cation in eight individual windows were used to generate the whole PMF, covering the entire reaction coordinate. The PMF data on both sides of the channel were further averaged to obtain better statistics, on the grounds of the symmetry of a CPNT.

RESULTS AND DISCUSSION

PMF Profiles of Ca^{2+}, K^+, and Na^+ Moving through CPNTs. Figure 2 illustrates the respective PMF profiles for a single Ca^{2+}, K^+, and Na^+ moving through the octa- and deca-CPNTs, obtained from ABF simulations. Overall, a small increase in the channel radius effectively reduces the free-energy barrier for cation transport through a water-filled channel, especially for Ca^{2+}. Such a change lowers the barrier for Ca^{2+} from ∼35 kcal/mol in the octa-CPNT to ∼10 kcal/mol in the deca-CPNT. The PMF curve of Ca^{2+} exhibits significant differences from those of Na^+ and K^+, featuring huge energy barriers in the centers of two CPNTs. In particular, for Ca^{2+} in the octa-CPNT, such a huge energy barrier makes it hard for Ca^{2+} to stay in the channel, which was well demonstrated by the random walk of Ca^{2+} in the tube, in which Ca^{2+} was found to run out of the tube about 5 ns later. Different from the PMF profile of Ca^{2+}, the free energies for Na^+ and K^+ at the mouths of two CPNTs are higher than those inside the tubes, indicating that Na^+ and K^+ can be trapped inside the tubes, especially inside the deca-CPNT.

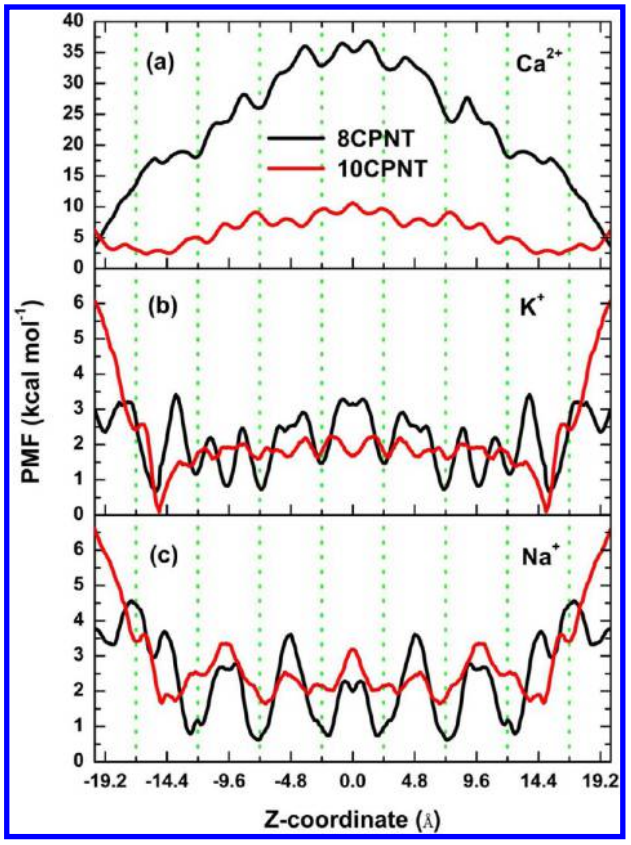

Figure 2. PMF profiles of a single Ca^{2+} (a), K^+ (b), and Na^+ (c) moving through the water-filled octa- (black) and deca-CPNTs (red). The vertical dashed lines represent the positions of dividual CP subunits. The z-axis was positioned along the major axis of a CPNT.

When moving through the octa-CPNT, Na^+ faces the highest energy barrier of ∼3.5 kcal/mol in the regions of gaps 3 and 5. For K^+, the highest energy barrier of ∼3.4 kcal/mol arises in the regions of gaps 1 and 7. The result that the highest energy barrier for K^+ is similar to that for Na^+ is consistent with the study by Hwang et al.,[23] who discovered that K^+ has the same dielectric barrier energy as Na^+ when entering a CPNT formed by four cyclo-[(D-Ala-Glu-D-Ala-Gln)$_2$-] subunits. Such entry barriers are not too high for Na^+ and K^+ to overcome, meaning that Na^+ and K^+ can both move across the octa-CPNT. The energy barriers for Na^+ and K^+ transporting through the deca-CPNT are much lower.

The PMF profiles of Na^+ and K^+ exhibit some analogous features. The free-energy landscapes between the second and seventh CP subunits (approximately -12 Å $\leq z \leq$ 12 Å) reflect the geometries of two CPNTs. Local maxima occurring in midplane regions and minima arising in α-plane zones result mainly from the regular and periodic arrangements of the composed CP subunits of two CPNTs.

Although a lot of similarities were seen in the PMF curves of Na^+ and K^+, some subtle differences also merit attention. First, Na^+ encounters slightly deeper energy wells than K^+ on the journey from the second to the seventh CP subunits, indicating that Na^+ may be trapped longer than K^+ in two CPNTs. The mild fluctuation of the free energy of K^+ in the deca-CPNT indicates that K^+ can move more freely in the channel. Second, compared with the energy barriers of Na^+ at $z = \pm 9.6$ Å (gaps 2 and 6) in the octa-CPNT, the PMF curve of K^+ presents energy wells there. Such an energy well has once been reported by Dehez et al.,[29] who mentioned that a markedly weaker minimum on the free-energy surface could occur when Na^+ locates equidistantly from two contiguous cyclic peptides. Interestingly, such weaker minima have not been found for Na^+ in the octa-CPNT, and only one in the first and last gaps of the deca-CPNT, respectively. Nevertheless, for K^+, such weaker minima arise in several gaps of the octa-CPNT and much more in the deca-CPNT.

Van der Waals and Electrostatic Interactions of Ca^{2+}, K^+, and Na^+ with a CPNT Wall and Channel Water. The vdW and electrostatic interactions of a cation with the framework of a CPNT and neighboring water molecules have been computed. To do so, the studied cation was fixed at the positions of $z = -24.0, -21.6, -19.2, \ldots, 19.2, 21.6$, and 24.0 Å along a tube axis (z-axis), respectively. The interval of adjacent sampling sites is 2.4 Å. A simulation of 2 ns with a time step of 1 fs was performed for each sampling site. The first 1 ns was for equilibration, and the last 1-ns trajectories were collected for data analysis. The results for Ca^{2+}, K^+, and Na^+ moving through two CPNTs are collectively depicted in Figure 3. Compared to the marked contribution of the electrostatic interaction energy to the total energy, the vdW interactions of a cation with a tube wall and water molecules are relatively weak and change little along the major axis of a CPNT. In particular, the electrostatic energy for the interaction of a cation with water molecules plays a determinant role.

DOI: 10.1021/acs.jcim.5b00025
J. Chem. Inf. Model. 2015, 55, 998−1011

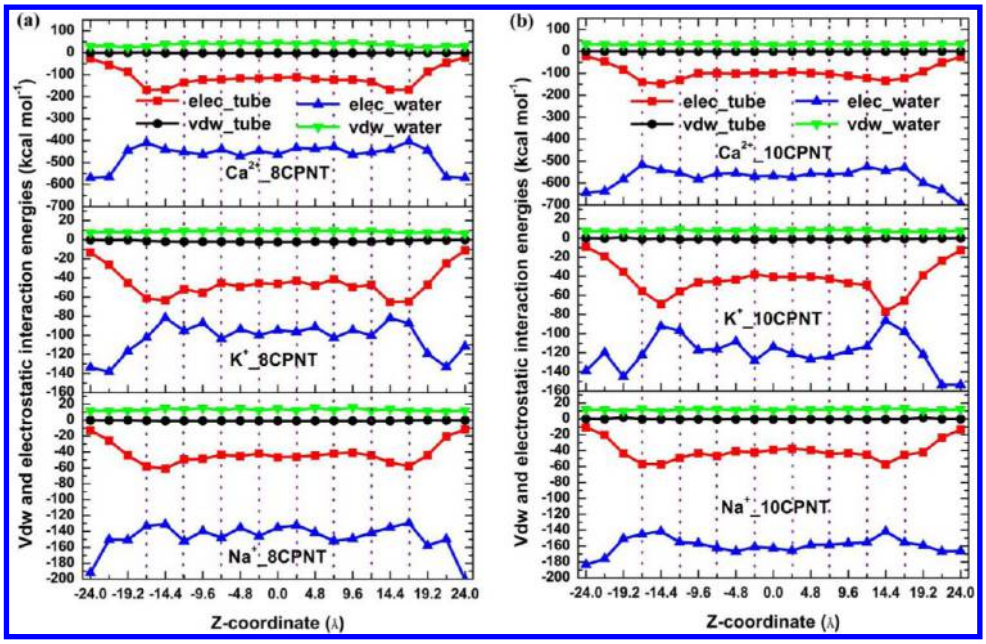

Figure 3. Van der Waals and electrostatic interactions of Ca^{2+}, K^+, and Na^+ in the water-filled octa- (a) and deca-CPNTs (b). The vdW and electrostatic interactions with water are represented by green and blue triangled lines, respectively. Those with the tube walls are represented by black circled and red squared lines, respectively. Vertical dashed lines represent the positions of dividual CP subunits.

As a cation enters a CPNT from a water solution, the electrostatic interaction energy between the cation and water molecules gradually weakens, while that between the cation and the tube becomes stronger. Obviously, due to the charge difference, the electrostatic energy for the interaction of Ca^{2+} with water molecules is significantly higher than those of K^+ and Na^+, and becomes stronger with increasing channel radius, due to more neighboring water molecules available there. On the contrary, the electrostatic energy for the interaction of Ca^{2+} with the framework of the deca-CPNT becomes lower, ascribed to the relatively longer distance between Ca^{2+} and the tube wall. But for Na^+ and K^+, the electrostatic energies for the interactions with both the octa- and deca-CPNTs show only tiny differences. Nevertheless, the electrostatic energies for the interactions of Na^+ and K^+ with water molecules have obvious differences, which can be ascribed to their different bulk solvation free energies.

Interaction Modes of Ca^{2+}, K^+, and Na^+ with the CPNTs. A cation can interact with the backbone of a CPNT by forming direct coordinations (DCs) and/or water bridges (WBs). WBs have been investigated to explore the transport mechanisms of small molecules, such as 5-fluorouracil, NH_3, CO_2, and O_2 through a CPNT.[45−47] In this study, we have investigated two interaction modes of Ca^{2+}, K^+, and Na^+ with the carbonyl oxygen ($O_{C=O}$) atoms of the octa- and deca-CPNTs by analyzing the trajectory of a 20-ns SMD simulation, respectively. The DCs were counted based on the positions of carbonyl oxygen atoms within the first shell of a cation (the radii are 3.0, 3.5, and 3.1 Å for Ca^{2+}, K^+, and Na^+, respectively). The definition of a WB, i.e., a water-mediated H-bonded interaction of a cation with the backbone $O_{C=O}$ of a CPNT, includes a critical distance of no longer than 3 Å between H_W (H of water) and $O_{C=O}$, and an angle of larger than 160° formed by O_W (O of water), H_W, and $O_{C=O}$ atoms. Besides, the involved water molecule should be within the first solvation shell of the cation.

A WB between a cation and a carbonyl oxygen ($O_{C=O}$) atom of a CPNT may associate with one, two, three, four, or even more water molecules. As an example, Figure s1 in the Supporting Information gives the results for the system with Ca^{2+} in the octa-CPNT. For Ca^{2+}, the WBs associated with one water molecule account for 86.68% and 75.04% in the octa- and deca-CPNTs, respectively. These percentages are 82.79% and 87.07% for K^+, and become 84.03% and 76.73% for Na^+ in the octa- and deca-CPNTs, respectively.

The numbers of WBs and DCs formed between a cation and the carbonyl oxygen ($O_{C=O}$) atoms of the octa- and deca-CPNTs during the pulling process of a 20-ns SMD simulation, respectively, are shown in Figure 4. It should be noted that the number of WBs mediated by only one water molecule was counted here, in consideration of low probabilities of WBs composed of more than one water molecule.

Obviously, as shown in Figure 4, much more WBs occur in the Ca^{2+} system; i.e., the WB-mediated interactions dominate the binding between Ca^{2+} and a CPNT, which is closely related to the strong hydration ability of Ca^{2+}. It can be found that a single Ca^{2+} can form at most seven WBs in the octa-CPNT. In comparison, the DCs between Ca^{2+} and the framework of a CPNT account for a small proportion. No more than three DCs were found for Ca^{2+} in the octa-CPNT, and Ca^{2+} rarely interacts with the wall of the deca-CPNT by DCs because of the long distance between them. Very few DCs sporadically arise in the vicinities of both ends of the deca-CPNT.

For the K^+ system, it can be found that K^+ can interact with the carbonyl oxygen atoms by more DCs than Na^+ and Ca^{2+} in both of two CPNTs. Similar phenomenon can be found in NavAb. Corry et al.[16] found that K^+, with a relatively larger ionic radius, tends to interact with the glutamate side chains by DCs, while the smaller ionic radius of Na^+ creates a preference for Na^+ interacting with the carboxylate groups through WBs. Computations of the average numbers of carbonyl oxygen atoms involved in forming DCs and WBs with K^+ give 1.7 and 0.6 in the octa-CPNT and 0.66 and 0.76 in the deca-CPNT,

DOI: 10.1021/acs.jcim.5b00025
J. Chem. Inf. Model. 2015, 55, 998−1011

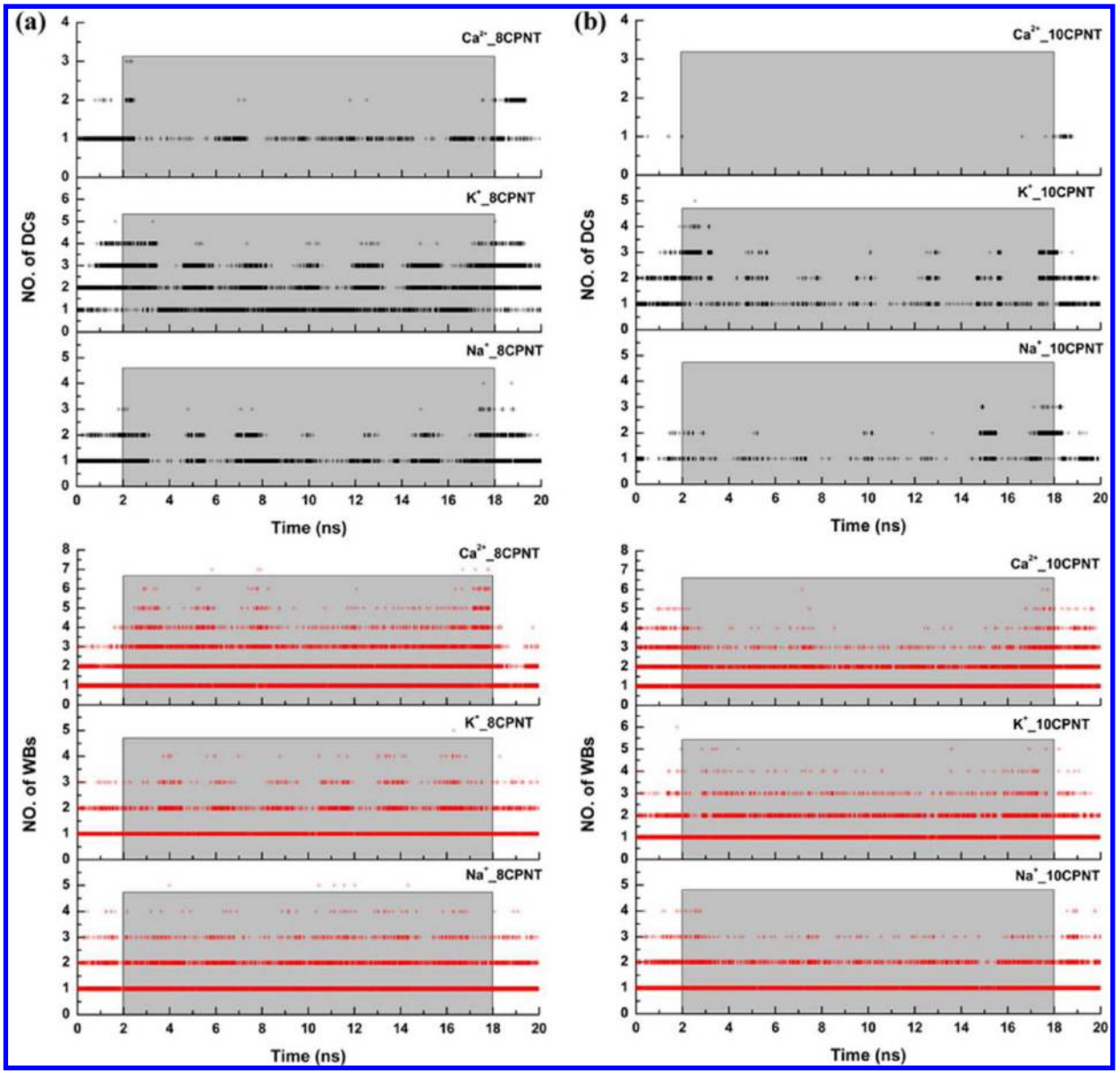

Figure 4. Time evolutions of the numbers of direct coordinations (DCs, black lines) and water bridges (WBs, red lines) formed between Ca^{2+}, K^+, and Na^+ and the frameworks of the octa- (a) and deca-CPNTs (b) during the pulling process of a 20-ns SMD simulation. The nanotube zones are shown by the light gray backgrounds.

respectively. Obviously, K^+ mainly interacts with the carbonyl oxygen ($O_{C=O}$) atoms by DCs in the narrower octa-CPNT, but these two types of interactions are almost evenly matched in the wider deca-CPNT.

The numbers of WBs and DCs for Na^+ interacting with the carbonyl oxygen ($O_{C=O}$) atoms of the octa- and deca-CPNTs are depicted in Figure 4. The average numbers of forming DCs and WBs are 0.59 and 0.64 for Na^+ in the octa-CPNT, 0.32 and 0.63 in the deca-CPNT, respectively. Obiviously, WBs contribute more to the $Na^+-O_{C=O}$ interaction than DCs in the wider deca-CPNT, but these two types of interactions are almost evenly matched in the narrower octa-CPNT.

Radial Distributions of Ca^{2+}, K^+, and Na^+ in Two CPNTs. In order to further clarify the interaction modes between a cation and its surroundings, the radial distributions of a cation, channel water oxygen (O_W), and carbonyl oxygen ($O_{C=O}$) atoms of a CPNT were investigated. To do so, a studied cation was initially fixed at the center of a CPNT for a 2-ns equilibrium and later allowed to move freely without any restraint for a 20-ns MD simulation in a NVT ensemble. It should be noted that the simulation time was increased to 30 ns for the random walks of Na^+ and K^+ in the octa-CPNT due to their slow moving. The results are collectively shown in Figure 5, where the physical quantity r denotes the distance of a species from the major axis of a CPNT and is calculated according to the formula: $r = (x^2 + y^2)^{1/2}$, in which the x and y coordinates of a species were used. It can be found that different cations leave the radial distributions of water and carbonyl oxygen (O_W and $O_{C=O}$) atoms basically unchanged. Concentric shells of water molecules are formed with common radial maxima at ca. 1.5 and 2.7 Å in the octa- and deca-CPNTs, respectively. As the channel radius increases, the water layer keeps almost an unchanged distance with the tube wall while gets away from a cation, which provides more space for a cation in the deca-CPNT.

DOI: 10.1021/acs.jcim.5b00025
J. Chem. Inf. Model. 2015, 55, 998−1011

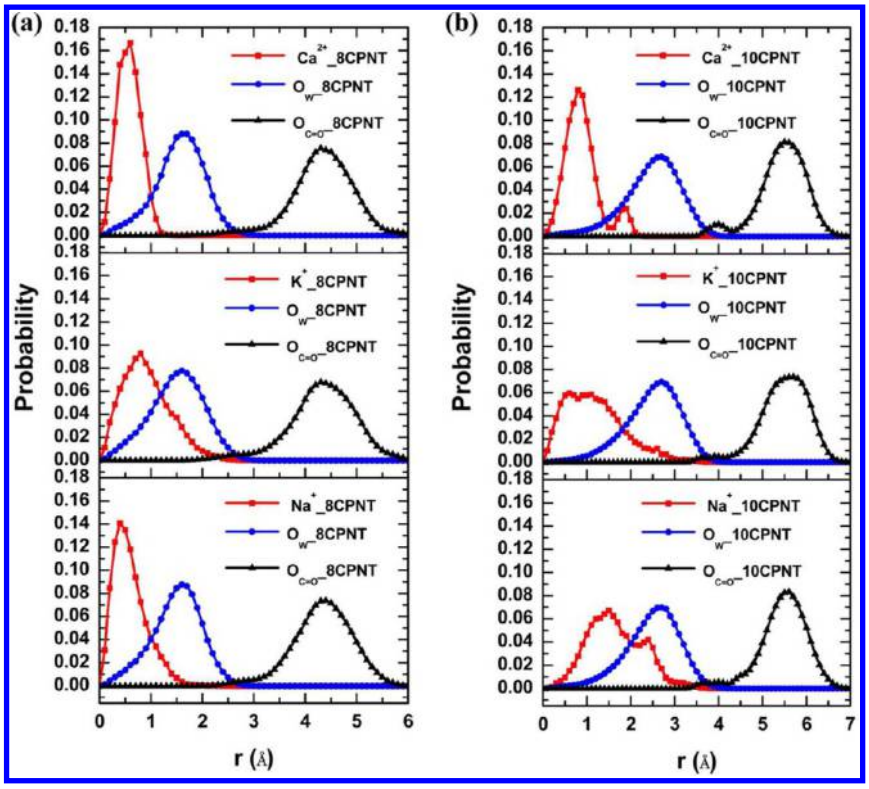

Figure 5. Radial distributions of Ca^{2+}, K^+, Na^+ (red), channel water O_W atoms (blue), and the carbonyl $O_{C=O}$ atoms (black) of the octa- (a) and deca-CPNTs (b).

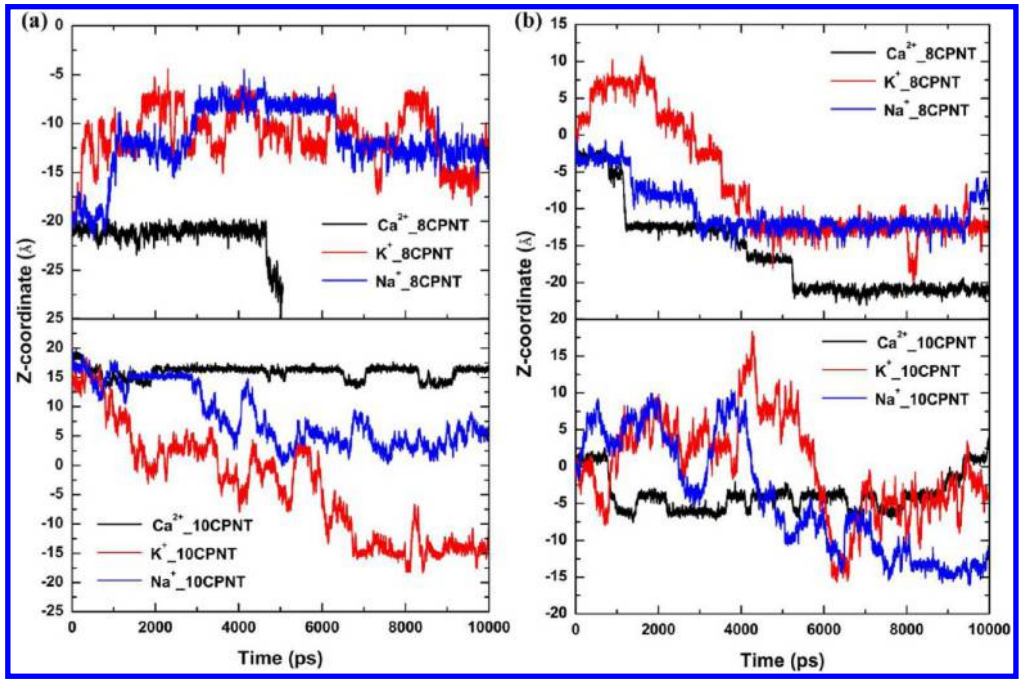

Figure 6. Time evolutions of the z-coordinates of a single Ca^{2+} (black), K^+ (red), and Na^+ (blue) initially introduced at the entrances ($z = \pm 20.0$ Å) (a) and the centers ($z = 0.0$ Å) (b) of the water-filled octa- and deca-CPNTs, obtained from ionic random walk MD simulations. The coverage intervals of the CPNTs along the z-axis are $[-16.8, +16.8]$.

Although Ca^{2+}, K^+, and Na^+ all prefer to reside near a tube axis, the distributions become broader as the channel radius increases. Relatively, Ca^{2+} prefers to reside near a tube axis more (Figure 5). Almost no overlapping between the profiles of Ca^{2+} and carbonyl oxygen ($O_{C=O}$) atoms indicates that Ca^{2+} hardly interact with the frameworks of the octa- and deca-CPNTs by DCs. As shown in Figure 5a, the K^+ distribution is relatively wider, slightly closer to the carbonyl oxygen ($O_{C=O}$) layer than Ca^{2+} and Na^+, leading to more DCs with the frameworks of two CPNTs than Ca^{2+} and Na^+. For Na^+ in the octa-CPNT, as shown in Figure 5a, the similarity of its radius to Ca^{2+} also leaves its radial distribution a clear peak at ~0.5 Å of

DOI: 10.1021/acs.jcim.5b00025
J. Chem. Inf. Model. 2015, 55, 998−1011

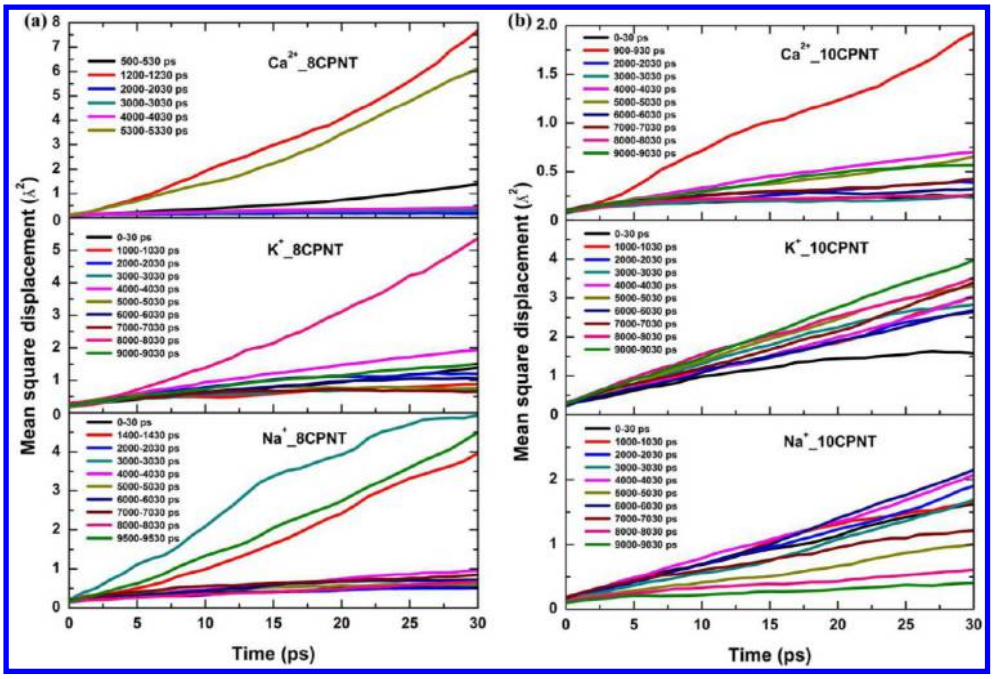

Figure 7. Time-dependent MSD_z curves of a single Ca^{2+}, K^+, and Na^+ along the z-axis (the major axis of a CPNT) inside the octa- (a) and deca-CPNTs (b) during different time periods.

the radial coordinate (r). While in the deca-CPNT, as shown in Figure 5b, the radial distribution profile for the Na^+ system exhibits some similarities with that for the K^+ system. But Na^+ is slightly closer to the channel water shell than K^+, indicating that Na^+ mainly interacts with the carbonyl oxygen ($O_{C=O}$) atoms by WB-mediated interactions in the deca-CPNT.

Axial Diffusions of Ca^{2+}, K^+, and Na^+ in Two CPNTs. Due to the complicated interactions with the surrounding, the movement of a cation is relevant with the ionic initial position. Taking into account the movement of a cation in a hydration state, analysis aims at the investigation of the ionic axial diffusion. Details with respect to the axial movements of Ca^{2+}, K^+, and Na^+ can be visualized from the time evolutions of the cations' z-coordinates, as depicted in Figure 6, obtained from the trajectories of the 10-ns random walk of a cation with an initial position at the entrance and center of a tube, respectively. It can be found that Ca^{2+} is unwilling to enter the channels, always staying in the water box and only visiting gap 7 of the deca-CPNT (Figure 6a). Nevertheless, K^+ and Na^+ can enter two CPNTs without too much hard (Figure 6a), due to the lower energy barriers (no higher than 3.0 kcal/mol) near the entrances (Figure 2b,c). In particular, K^+ behaves most actively and visits the whole deca-CPNT, no matter where the initial position is (Figure 6). Similar phenomenon can be found in the bacterial voltage-gated sodium channel NavAb. Ke et al.[14] once reported that Na^+ moved into the channel quickly (within ~5 ns), while Ca^{2+} wandered at the entrance of the channel for ~40 ns. Moreover, Ca^{2+}, with an initial position at the center of the octa-CPNT, was found to move quickly to the outside of the channel and only wander in a small region in the deca-CPNT, shown in Figure 6b.

The axial mobility of a cation in a CPNT can be described by the short-time local diffusion coefficient[5,48] of the cation along the major axis (z-axis) of the CPNT, which can be computed from the following equation:

$$D_z = \mathrm{MSD}_z(t)/2t = \frac{1}{2t}\left\langle \frac{1}{N}\sum_{i=0}^{N} |z_i(t) - z_i(0)|^2 \right\rangle \quad (1)$$

where $z_i(t) - z_i(0)$ is the axial distance traveled by species i over the time interval t, and the angle brackets denote the ensemble average over many time intervals and over all the species in the channel (N). Here, the species i denotes to a single Ca^{2+}, K^+, and Na^+, respectively. The $MSD_z \sim t$ curves at different time periods are calculated and plotted in Figure 7. According to the slopes of the $MSD_z \sim t$ curves, the axial diffusion coefficients (D_z) of Ca^{2+}, K^+, and Na^+ at different time periods can be obtained. It is worth noting that Ca^{2+} drifts rapidly at the time periods of 1200−1230 and 5300−5330 ps with D_z = 121.90 and 101.64 Å^2 ns^{-1}, respectively. Based on the trajectories of Ca^{2+} in the octa-CPNT, shown in Figure 6b, it can be found that Ca^{2+} is attempting to leave from gap 3 to gap 1 and escape from the tube to the water box at these two periods, respectively. But, most of the time, Ca^{2+} moves slowly in the octa-CPNT, with $D_z \approx$ 1.5−5.0 Å^2 ns^{-1}. For K^+ in the octa-CPNT, the most rapid drift, with D_z = 85.45 Å^2 ns^{-1}, occurs at the time period of 8000−8030 ps, when K^+ is attempting to escape from the tube to the water box (it quickly returns to the tube later). Compared with Ca^{2+}, K^+ moves relatively quickly in most of the time, with $D_z \approx$ 6.0−28 Å^2 ns^{-1}. With respect to Na^+ in the octa-CPNT, three rapidest drifts occur at the time periods of 1400−1430, 3000−3030, and 9500−9530 ps with D_z = 66.73, 86.16, and 72.82 Å^2 ns^{-1}, when Na^+ is trying to jump from gap 3 to gap 2, from gap 2 to gap 1, and return to gap 2 from gap 1, respectively. Compared with Ca^{2+} and K^+, most of the time, Na^+ moves moderately in the octa-CPNT, with $D_z \approx$ 5.6−13 Å^2 ns^{-1}.

Things become quite different in the deca-CPNT. For K^+ and Na^+, ultrafast drifts are rare, and on the average, the two cations move quickly, with $D_z \approx$ 39.0−62.0 and 14.0−30.0 Å^2 ns^{-1}, respectively, due to their relatively smooth PMF in the deca-CPNT, shown in Figure 2. For Ca^{2+}, the rapid drift with

DOI: 10.1021/acs.jcim.5b00025
J. Chem. Inf. Model. 2015, 55, 998−1011

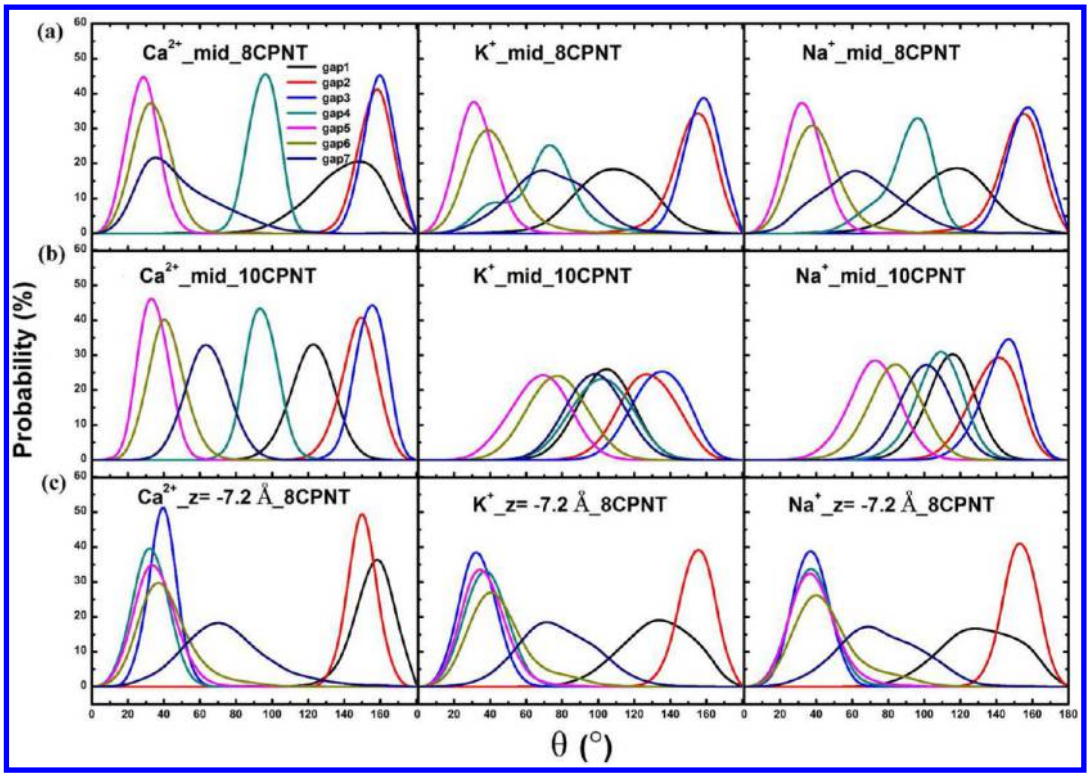

Figure 8. Probability distributions of the dipole orientation angles (θ) of channel water molecules when a single Ca^{2+}, K^+, and Na^+ locates at the centers of the octa- (a) and the deca-CPNTs (b). Those when Ca^{2+}, K^+, and Na^+ locate at the position of $z = -7.2$ Å (an α-plane zone) of the octa-CPNT are illustrated in (c).

D_z = 29.67 Å^2 ns^{-1} occurs at the time period of 900−930 ps, when Ca^{2+} is attempting to jump from gap 4 (center of the tube) to gap 3. But, most of the time, Ca^{2+} moves slowly, with $D_z \approx 2.5-10.0$ Å^2 ns^{-1}.

Influences of Ca^{2+}, K^+, and Na^+ on the Dipole Orientations of Channel Water. The dipole orientation change of water molecules in a nanotube was considered to be one of the important affects of the incorporation of an ion on channel water movement. Zhou et al.[49] once proposed a parameter named "hydration factor" to investigate channel water dipole orientation quantitatively. Here, to describe water dipole orientation, θ was defined as the angle between the dipole of a channel water molecule and a CPNT axis (z-axis). When a cation exists in a CPNT, water oxygen atoms in the vicinity of the cation inevitably face toward the ion, and the hydrogen atoms are prone to stay away. Figure 8 illustrates the distribution profiles of θ in dividual gaps for a single Ca^{2+}, K^+, and Na^+ locating at the center or an α-plane zone ($z = -7.2$ Å) inside two CPNTs. For comparison, the results for pristine CPNTs (without any ions) are depicted in Figure s2 in the Supporting Information.

Compared with the profiles without any ions in the octa-CPNT (Figure s2a),[35] it can be found that the incorporation of a single Ca^{2+}, K^+, and Na^+ in the center (gap 4) of the tube, respectively, makes the water molecules in the neighboring gaps 2, 3, 5, and 6 possess strong orientations, indicated by the peaks at ∼30° and 160° of θ. It is resulted from the strong electrostatic interactions with the cations. The highest peaks indicate that Ca^{2+} has the strongest effect on the dipole orientations of channel water molecules due to its +2 ionic state. Water molecules in gap 4 where a cation exists present sharp peaks at ∼95°, 75°, and 95° of θ for the systems containing Ca^{2+}, K^+, and Na^+, respectively. The number of water molecules in gap 4 (-2.4 Å $\le z \le 2.4$ Å) gives rise to this difference. When a single K^+ which has a relatively larger ionic radius (1.5 Å) exists in gap 4, this region can only accommodate three water molecules on the average, while average numbers of water molecules in gap 4 become 6 and 4 for the Ca^{2+} and Na^+ systems, respectively. As shown in Figure s3 in the Supporting Information, for the Ca^{2+} and Na^+ systems, the "+dipole" states ($0° < \theta < 90°$) and "−dipole" states ($90° < \theta < 180°$) of water molecules in gap 4 always come in pairs, while the two states do not feel evenly matched for the K^+ system.

Figure 8a indicates that the channel water molecules in two end gaps (gaps 1 and 7) present wide distributions of dipole orientations. When Ca^{2+} locates at the center of the octa-CPNT, the relatively narrower peaks in gaps 1 and 7 indicate channel water molecules there have relatively stronger dipole orientations. But for the systems containing Na^+ or K^+, H-bond defects are more likely to exist in these regions, associated with 90° of the orientation angles (θ). Usually, H-bond defects can be divided into "L-defects" and "D-defects". An L-defect occurs when a water molecule in a H-bonded chain simultaneously serves as a H donor to its two adjacent water molecules, while it acts as a receptor in a D-defect. Water molecules in two end gaps simultaneously suffer two orientation affects. One from the negative carbonyl groups at two ends of a CPNT induces the dipole orientations of neighboring water molecules to point to the center of the tube. Another from a cation in the channel makes the dipole orientations of water molecules point away from the ion. Such two opposite orientation affects both try to transfer forward through water chain and meet together in gaps 1 and 7, resulting in H-bond defects there. Here, only D-defects

DOI: 10.1021/acs.jcim.5b00025
J. Chem. Inf. Model. 2015, 55, 998−1011

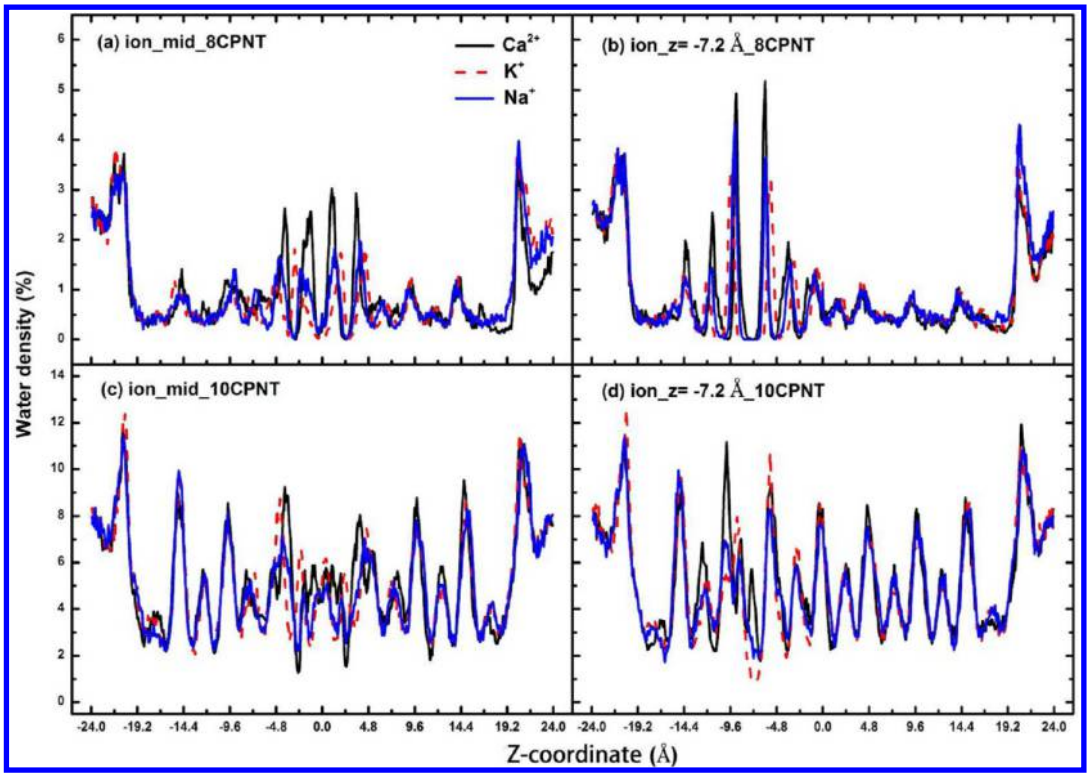

Figure 9. Axial distributions of water molecules inside the octa- (a,b) and deca-CPNTs (c,d) with a single Ca^{2+} (black solid lines), K^+ (red dashed lines), and Na^+ (blue solid lines) locating at the centers and at the positions of $z = -7.2$ Å of the tubes, respectively.

were found by analyzing the trajectories of a 10-ns MD simulation. Nevertheless, *L*-defects were once reported for a charged CNT.[50] For the systems containing a single Ca^{2+}, K^+, and Na^+ in the octa-CPNT, the percentages of *D*-defects reach 0.84%, 12.65%, and 8.76%, respectively, indicating that *D*-defects are most likely to arise under the presence of K^+.

Results in the deca-CPNT show sharp differences with those in the octa-CPNT. All the distribution curves distinctly move toward 90° of θ, especially in gaps 4, 1, and 7, which is resulted from the water molecular configurations there. As the channel radius increases, water molecules in gap 4 of the deca-CPNT distribute around a cation more symmetrically due to the larger available space. Thus, the "+dipole" states and "−dipole" states are more likely to arise in pairs, causing the distribution in gap 4 to move toward 90° of θ. As mentioned above, the dipole orientations of water molecules in gaps 1 and 7 can be influenced by two competing orientation affects, one from the bare carbonyl groups at the ends of a CPNT and another from the introduced cation in the channel. On one hand, more bare carbonyl groups exist in the deca-CPNT, enhancing the affects on the dipole orientations of water molecules. On the other hand, the impact of the cation weakens due to the larger interior space of the deca-CPNT. As a result, much more *D*-defects were formed in gaps 1 and 7 of the deca-CPNT. The percentages reach 2.25%, 22.85%, and 20.57% for the Ca^{2+}, K^+, and Na^+ systems, respectively.

Significant differences can be generated on the dipole orientations of water molecules in dividual gaps due to the position change of a cation. Li et al.[7] once reported that the dipole moment distributions of channel water relied on the location of K^+ in the GA channel. They found that water alignment was essentially perfect once a single K^+ was in the inner binding site. Figure 8c illustrates the distributions of θ in dividual gaps of the octa-CPNT with a cation locating at the position of $z = -7.2$ Å (an α-plane zone), closer to gap 1 but a little farther to gap 7. Overall, the distribution curves for the systems containing Ca^{2+}, K^+, and Na^+ present similar shape features except in gap 1. As described above, *D*-defects may occur in two end gaps. But, for the Ca^{2+} system, the peak at 160° suggests that water molecules in gap 1 have strong dipole orientations while only in gap 7 can a H-bond defect occur. This implies that the dipole orientations of water molecules in gap 1 have been totally regulated by Ca^{2+} due to the closer distance. With regard to the Na^+ and K^+ systems, *D*-defects can both appear in gaps 1 and 7. The probabilities of the H-bond defects in these two gaps vary widely. Only 3.02% and 2.06% in gap 1 were found for the Na^+ and K^+ systems, respectively, while in gap 7, these percentages significantly increase to 12.98% and 14.17%, respectively.

Influences of Ca^{2+}, K^+, and Na^+ on the Axial Distribution of Channel Water. Not only did the existence of a cation affect the dipole orientations of water molecules in a nanotube, it could change the original water-chain structure in the tube. Thus, the axial density distributions of water molecules inside the octa- and deca-CPNTs with the incorporation of a single Ca^{2+}, K^+, or Na^+ in the center and an α-plane zone ($z = -7.2$ Å) along the tube axes (z-axes) were calculated, respectively, and are collectively depicted in Figure 9. As we expected, the configuration of channel water in the octa-CPNT no longer presents the regular form of a 1-2-1-2 file. It can be found that four high peaks arise around a cation locating in the center of the channel ($z = 0$ Å), and two extremely high peaks and four moderate ones around a cation locating at the position of $z = -7.2$ Å (an α-plane zone). Such differences result from the different available water molecules around a cation. When a cation locates in a midplane region,

DOI: 10.1021/acs.jcim.5b00025
J. Chem. Inf. Model. 2015, 55, 998−1011

fewer water molecules in the neighboring α-plane zones can get around the ion due to the space limitation. However, when a cation locates in an α-plane zone, more water molecules available in the neighboring midplane regions due to larger space there, thus resulting in two extremely high peaks in Figure 9b. The strongest attraction between water molecules and Ca^{2+} induces most water molecules to gather around Ca^{2+}, forming the highest peaks in Figure 9a,b, compared with the results in the K^+ and Na^+ systems.

Furthermore, the average numbers of water molecules in the first and second solvation shells of Ca^{2+}, K^+, and Na^+ locating in an α-plane zone and midplane region of the octa-CPNT have been calculated, respectively. In total, 6 and 4 water molecules are found in the first and second solvation shells of Ca^{2+} locating in an α-plane of the octa-CPNT. Those for Ca^{2+} locating in a midplane region give 6 and 5.5, respectively. For K^+ in an α-plane zone, on average 4.9 and 2.5 water molecules were found in the first and second shells, but 3.8 and 4 in a midplane region, respectively. For Na^+ in an α-plane, the results are 4.9 in the first shell and 2.7 in the second shell, but 4.1 and 4.1 for Na^+ in a midplane region, respectively. It can be found that, when a cation locates in a midplane region, there is no distinct difference between the average numbers of water molecules in the first and second solvation shells of the ion, resulting in four peaks with similar heights around the ion in Figure 9a. When a cation locates in an α-plane zone, two more water molecules in the first solvation shell than in the second one were found, inducing two peaks specially high around the ion. Nevertheless, when a cation locates in the deca-CPNT, all the significant peaks disappear, resulted from the bulk-like water structure in the deca-CPNT.

Influences of Ca^{2+}, K^+, and Na^+ on the Axial Diffusion of Channel Water. The introduction of a cation inside a CPNT can inevitably influence the movement of channel water. Here, trajectory analysis mainly aims at the investigation of the axial diffusion coefficient (D_z) of channel water in two CPNTs, with a cation first introduced in the center of a CPNT and later allowed to move freely. The results computed from eq 1 are collectively illustrated in Figure 10. The good linearity of the $MSD_z \sim t$ curves indicates that the axial movement of channel water still keeps one-dimensional diffusion under the implantation of a cation. According to the slopes of the $MSD_z \sim t$ curves, the axial diffusion coefficients (D_z) of water molecules in the octa-CPNT were computed to be 7.75, 35.61, and 15.97 $Å^2\ ns^{-1}$ in the Ca^{2+}, K^+, and Na^+ systems, respectively. Those in the deca-CPNT give the values of 19.75, 49.39, and 34.3 $Å^2\ ns^{-1}$ in the Ca^{2+}, K^+, and Na^+ systems, respectively. The D_z values of channel water in two CPNTs increase in the order of the Ca^{2+}, Na^+, and K^+ systems. The results indicate that the more attractive an implanted cation is, the slower channel water molecules move.

Compared with our previous results (62 and 130 $Å^2\ ns^{-1}$ of the water axial diffusion coefficients (D_z) in the octa- and deca-CPNTs, respectively), obtained from a similar system without any ions,[3] it can be deduced that the introduction of a cation may exert a great influence upon the movement of channel water in a CPNT. The strong electrostatic interaction with a cation largely reduces the diffusion of channel water. As a divalent cation, Ca^{2+} exerts the strongest interaction with water molecules. Na^+ has a smaller radius, compared with K^+, and shows moderate interaction with water.

Hydrations of Ca^{2+}, K^+, and Na^+ in Two CPNTs. A standard method, for studying the structures of water molecules around a cation confined in a CPNT, is to calculate the cation−oxygen (O_W) radial distribution function (RDF). The results for Ca^{2+}, K^+, and Na^+ in the octa- and deca-CPNTs, obtained from the trajectories of the random walk MD simulations of these cations, are collectively plotted in Figure 11. There are always a very high peak and a low one for each profile, indicating two water solvation shells of each cation inside two CPNTs. The first peaks for the Ca^{2+}, K^+, and Na^+ systems locate at the positions of 2.25, 2.65, and 2.25 Å of the distance (r) between a cation and O_W, respectively. Ionic charge and radius can both influence the strength of the first peak. Ca^{2+}, a divalent cation, gives the highest of the first peak. The ionic radius of Na^+ is much smaller than that of K^+, giving a more pronounced first peak of the Na^+−oxygen RDF, compared with the K^+−oxygen RDF.

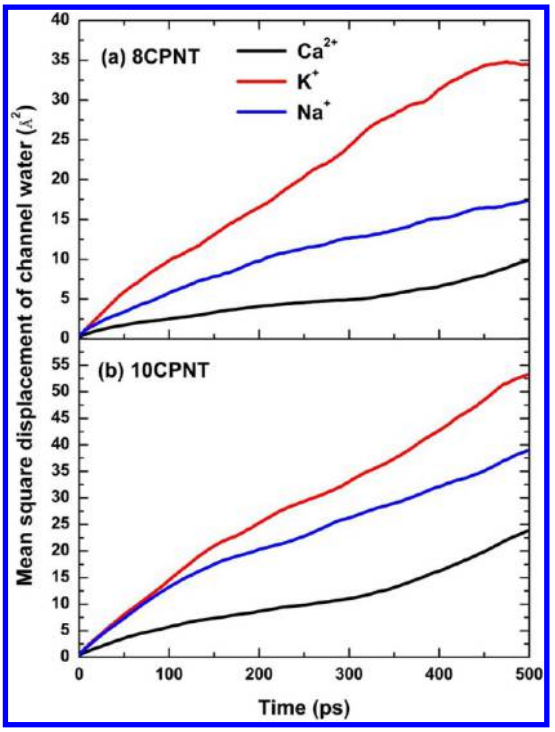

Figure 10. Time-dependent MSD_z curves of channel water molecules along the z-axis (the major axis of a CPNT) inside the octa- (a) and deca-CPNTs (b) with a single Ca^{2+} (black), K^+ (red), and Na^+ (blue) initially implanted at the center of a CPNT and allowed to walk randomly inside the channel.

The numeric integration of a cation-oxygen O_W RDF can give the number of solvation water molecules around a cation. The results of the average numbers of water molecules in the first (SN_1) and second (SN_2) solvation shells of Ca^{2+}, K^+, and Na^+ in the octa-CPNT, deca-CPNT, and bulk are included in Table 1. Compared with the results in bulk, no significant changes of SN_1 for Ca^{2+} and Na^+ in the octa- and deca-CPNTs indicate that the first solvation shells of Ca^{2+} and Na^+ are basically saturated with water molecules in these two confined CPNTs, mainly due to the small ionic radii of Ca^{2+} and Na^+. It is difficult for the first solvation shell of K^+ to saturate with water molecules in the octa-CPNT, due to the relatively larger radius of K^+ and limited interior space of the octa-CPNT. Nevertheless, the first solvation shell of K^+ is nearly saturated in the deca-CPNT, where more water molecules are available.

As the channel radius increases, the second peaks in cation-oxygen (O_W) RDFs slightly shift to the right (see r_2 in Table 1),

DOI: 10.1021/acs.jcim.5b00025
J. Chem. Inf. Model. 2015, 55, 998−1011

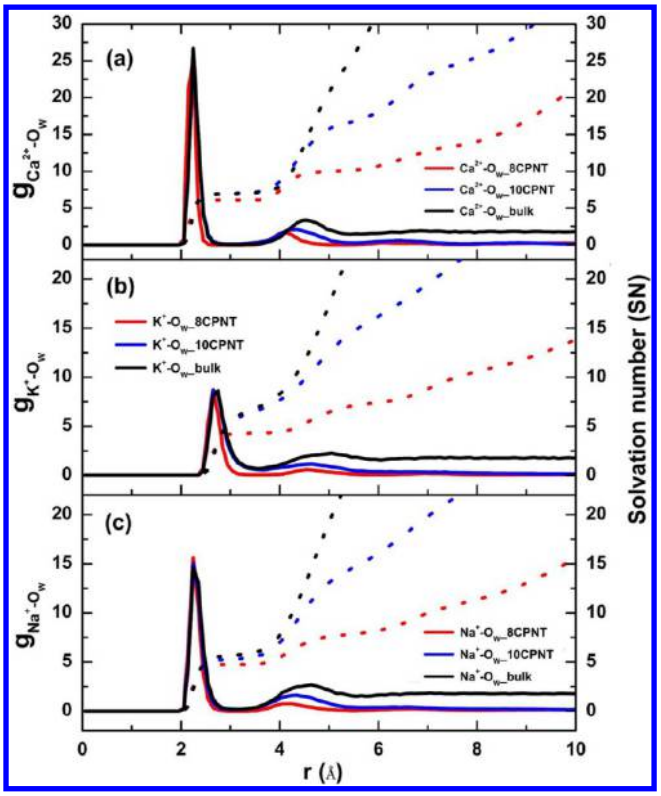

Figure 11. Radial distribution functions between cations and water O_W atoms when a single Ca^{2+} (a), K^+ (b), and Na^+ (c) randomly walk inside the water-filled octa-CPNT (red), deca-CPNT (blue), and bulk solution (black). The integration curves of the RDF profiles are also included and shown in dotted red, blue and black lines, respectively.

and their heights obviously increase, indicating more water molecules in the second shells (SN_2) of cations. Nevertheless, compared with the results in bulk, it is hard for the second solvation shells of these cations to be saturated with water molecules, mainly due to the spatial constraints of two CPNTs.

Compared with Na^+ and K^+, the water solvation number (SN_1) in the first shell of Ca^{2+} is the largest in both octa- and deca-CPNTs. Especially in the wider deca-CPNT, SN_1 of Ca^{2+} is almost equal to that in bulk, due to its small ionic radius and strong hydration ability. With respect to K^+, the hydration is incomplete due to its larger ionic radius. Especially in the octa-CPNT, SN_1 of K^+ is only 4.3. It can be found that, in the narrower octa-CPNT, SN_1 of Na^+ is larger than that of K^+, which is mainly ascribed to the smaller size of Na^+. On the contrary, in the wider deca-CPNT, SN_1 of K^+ is larger than that of Na^+, due to there being more water molecules available and the relatively stronger solvation ability of K^+.

The change of the ionic hydration for a cation moving through a CPNT can be visualized from the plots of the time evolutions of cation−O_W distance and the number of the first-shell water molecules. Results for Ca^{2+}, K^+, and Na^+ are depicted in Figures 12−14, respectively. As shown in Figure

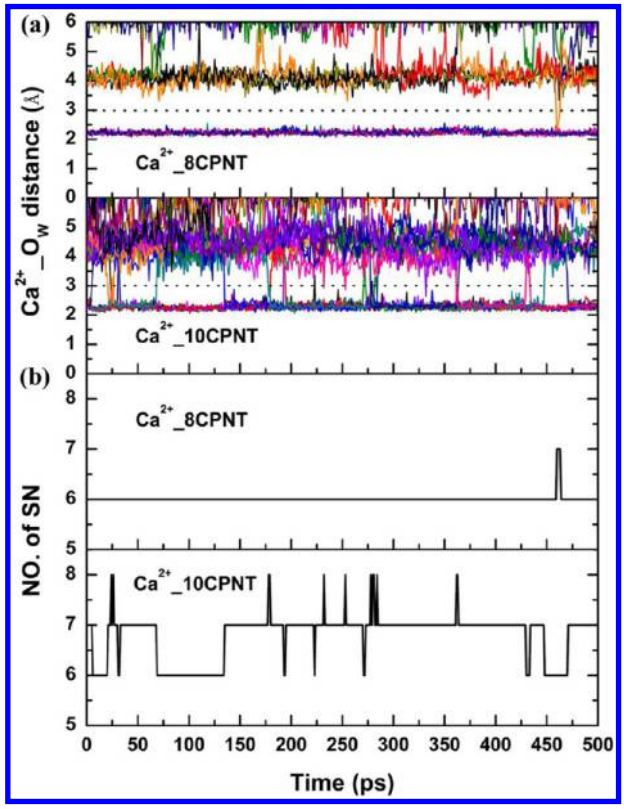

Figure 12. Time evolutions of Ca^{2+}−O_W distance (a) and the number of the first-shell water molecules (SN) of Ca^{2+} (b), obtained from the random walk MD simulations of Ca^{2+} in the water-filled octa- and deca-CPNTs. The dashed lines indicate the largest distances between Ca^{2+} and its directly coordinating water oxygen atoms, obtained from the first minimum of the Ca^{2+}−O_W RDFs in Figure 11.

12b, the complex species $[Ca(H_2O)_6]^{2+}$and $[Ca(H_2O)_8]^{2+}$ can be transiently formed from the most favorable $[Ca(H_2O)_7]^{2+}$ in the deca-CPNT, which leads to a small amount of interchange attempts between the first-shell water molecules and the ones in the outer region. Such interchange can be ascribed to the participation of carbonyl oxygen ($O_{C=O}$) atoms of the deca-CPNT and surrounding water molecules. For instance, Figure s4a in the Supporting Information shows that, at the simulation time of 192 ps, one (labeled in green) of the first-shell water molecules ran out of the shell, under the drag by another water molecule (labeled in purple) and one carbonyl oxygen ($O_{C=O}$)

Table 1. Positions of the First (r_1) and Second Maxima (r_2) of the Cation−Water Oxygen Radial Distribution Functions for Ca^{2+}, K^+, and Na^+ in the Octa- and Deca-CPNTs and the Average Water Solvation Numbers in the First (SN_1) and Second (SN_2) Solvation Shells of the Cations in Two CPNTs[a]

	Ca^{2+}				K^+				Na^+			
	r_1/Å	r_2/Å	SN_1	SN_2	r_1/Å	r_2/Å	SN_1	SN_2	r_1/Å	r_2/Å	SN_1	SN_2
octa-CPNT	2.25	4.05	6.1	3.9	2.65	4.55	4.3	3.1	2.25	4.25	4.7	3.2
deca-CPNT	2.25	4.35	6.9	9.8	2.65	4.65	6.6	10	2.25	4.35	5.3	9.7
bulk	2.25	4.55	6.9	18.4	2.65	5.05	6.9	24.1	2.25	4.65	5.7	19.6

[a]SN_1 and SN_2 were obtained from the trajectories of the random walk of a cation in the tube. The results for cations in bulk are also included.

DOI: 10.1021/acs.jcim.5b00025
J. Chem. Inf. Model. 2015, 55, 998−1011

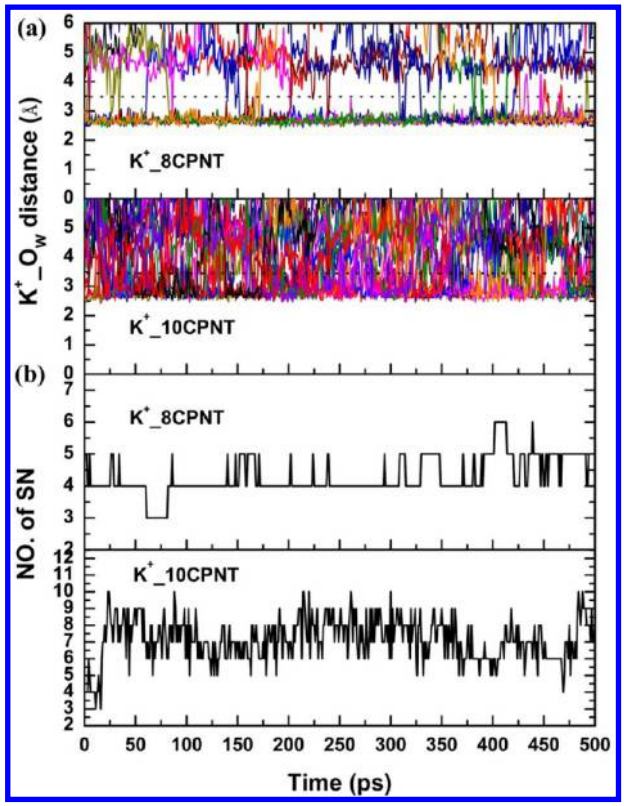

Figure 13. Time evolutions of K^+-O_W distance (a) and the number of the first-shell water molecules (SN) of K^+ (b), obtained from the random walk MD simulations of K^+ in the water-filled octa- and deca-CPNTs. The dashed lines indicate the largest distances between K^+ and its directly coordinating water oxygen atoms, obtained from the first minimum of the K^+-O_W RDFs in Figure 11.

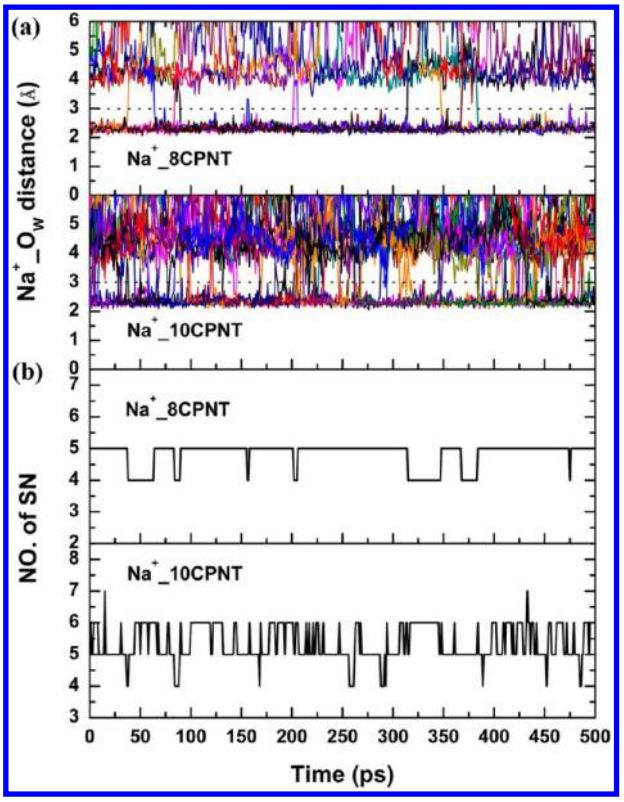

Figure 14. Time evolutions of Na^+-O_W distance (a) and the number of the first-shell water molecules (SN) of Na^+ (b), obtained from the random walk MD simulations of Na^+ in the water-filled octa- and deca-CPNTs. The dashed lines indicate the largest distances between Na^+ and its directly coordinating water oxygen atoms, obtained from the first minimum of the Na^+-O_W RDFs in Figure 11.

atom (labeled in yellow) by means of H-bonded interactions. Sometimes, such interchange did not change the number of water molecules in the first solvation shell of a cation. For example, Figure s4b illustrates that, at the simulation time of 355 ps, one water molecule (labeled in green) ran away from the first solvation shell of Ca^{2+}, and another one (labeled in brown) in the outer region tried to move in. In this way, although the water solvation number of the cation remains unchanged, the first-shell water molecules succeed in exchanging with the ambient. Nevertheless, such interchange is unusual in the octa-CPNT, as depicted in Figure 12, implying the $[Ca(H_2O)_6]^{2+}$ species is extremely stable in the channel. Furthermore, the combinations of the six water molecules in the first shell with Ca^{2+} in octa-CPNT keep for long time, verified from the time evolution of the cation−O distance around 2.2 Å.

For K^+, as shown in Figure 13, it is obvious that water molecules surrounding the cation are quite labile, showing numerous water exchange processes during the random walk MD simulation. Especially in the deca-CPNT, the solvation number of K^+ changes a great deal, ranging from 3 to 10. That in the octa-CPNT gives from 3 to 6. The average number of the first-shell water molecules in the octa-CPNT is less than that in the deca-CPNT, but more stable, verified from the time evolution of the cation−O distance in the channel. The $[K(H_2O)_4]^+$ and $[K(H_2O)_7]^+$ species are found to be dominant in the octa- and deca-CPNTs, respectively.

For Na^+, as shown in Figure 14, the solvation number of the first shell of Na^+ in the octa-CPNT is 4−5, and 4−7 in the deca-CPNT. The most favorable species in the octa-CPNT is $[Na(H_2O)_5]^+$, while $[Na(H_2O)_6]^+$ and $[Na(H_2O)_5]^+$ are found to be dominant species in the deca-CPNT. The exchange processes between the water molecules in the first solvation shell and the ones in the outer region happen occasionally, with a lower frequency than those in the K^+ system, verified from the time evolution of Na^+-O distance in the channel.

Overall, it is obvious that the first solvation shell of Ca^{2+} is most stable, while that of K^+ is most labile. Furthermore, the increase of the channel radius induces destabilization of the hydration shell, leading to numerous interchange attempts between the first-shell water molecules and the ones in the outer region.

■ CONCLUSION

The transport properties of Ca^{2+}, K^+, and Na^+ in two transmembrane CPNTs of 8 × $(WL)_{n=4,5}$/POPE have been investigated in detail. The following points have been concluded:

(1) PMF computations indicate that huge energy barriers at the mouths of the octa-CPNT keep Ca^{2+} out of the channel, while Na^+ and K^+ can be trapped inside these two CPNTs. Furthermore, Na^+ encounters deeper energy wells than K^+, and thus it can stay longer in the channels. An increase of the CPNT radius can effectively reduce the free energy barrier for a cation transporting through a water-filled CPNT, especially for Ca^{2+}.

DOI: 10.1021/acs.jcim.5b00025
J. Chem. Inf. Model. 2015, 55, 998−1011

(2) The electrostatic interaction of Ca^{2+} with channel water significantly increases with the augment of the channel radius, compared with those of K^+ and Na^+, due to its +2 ionic state.

(3) Analysis of radial distributions reveals that these cations prefer to reside near a tube axis. Water-bridged interactions were mostly found between Ca^{2+} and the framework of the octa-CPNT, and direct coordinations mostly occur for K^+ in the octa-CPNT. In the deca-CPNT, water-bridged interactions dominate the bindings between all the cations and the framework of the CPNT.

(4) The axial diffusion behavior of a cation is related to the ionic position. A cation may drift rapidly or behave lazily in a CPNT. K^+ behaves most actively and can visit the whole deca-CPNT quickly.

(5) The introduction of a cation significantly influences the dipole orientations and axial distribution of channel water, resulting in *D*-defects occurring in the first and last gaps, which are found most likely to arise in the presence of K^+. Moreover, the strong electrostatic interaction with a cation largely reduces the movement of channel water. The axial diffusion coefficients (D_z) of channel water in two CPNTs increase in the order of the Ca^{2+}, Na^+, and K^+ systems.

(6) Detailed analysis of ionic hydrations clearly shows that the first solvation shells of Ca^{2+} and Na^+ are basically saturated with water molecules in these two confined CPNTs, while the hydration of K^+ is substantially incomplete in the octa-CPNT. Furthermore, it was found that the first coordination shell of Ca^{2+} is most stable, especially in the octa-CPNT, while that of K^+ is most labile, especially in the deca-CPNT. Increasing the channel radius may induce instability of the ionic hydration shell, leading to numerous attempts of the first-shell water molecules of a cation to interchange with those in the outer region.

These points taken together, it is clear that the transport behavior of a cation not only depends on the radius of a CPNT, but also closely relates to the radius, charge, and hydration ability of the cation. The findings in this work reveal the transport behavior and mechanism for a cation moving through a water-filled transmembrane CPNT at an atomic level, providing relevant information for the research on an ion channel.

■ ASSOCIATED CONTENT

Supporting Information

Figure s1, water bridges composed of 1−6 mediated water molecules between Ca^{2+} and the carbonyl oxygen atoms of the octa-CPNT; Figure s2, probability distributions of the dipole orientation angles of channel water in the octa- and deca-CPNTs without any ions in the tubes; Figure s3, snapshots of water molecular configurations in gap 4 with a single Ca^{2+}, K^+, or Na^+ locating at the center of the water-filled octa-CPNT; and Figure s4, snapshots of two interchange modes between the first-shell water molecules of Ca^{2+} and surrounding water molecules in the deca-CPNT. The Supporting Information is available free of charge on the ACS Publications website at DOI: 10.1021/acs.jcim.5b00025.

■ AUTHOR INFORMATION

Corresponding Author

*Telephone: 0086-0512-65883271. E-mail: jffan1305@163.com.

Notes

The authors declare no competing financial interest.

■ ACKNOWLEDGMENTS

This work has been supported by the National Natural Science Foundation of China (Grant No. 21173154) and the Priority Academic Program Development of Jiangsu Higher Education Institutions. It was further supported by the National Basic Research Program of China (973 program, Grant No. 2012CBB25803). The authors are grateful to Mr. Jian Liu and Rui Li for their insightful suggestions.

■ REFERENCES

(1) Ghadiri, M. R.; Granja, J. R.; Milligan, R. A.; McRee, D. E.; Khazanovich, N. Self-assembling Organic Nanotubes Based on a Cyclic Peptide Architecture. *Nature* **1993**, *366*, 324−327.

(2) García-Fandiño, R.; Granja, J. R.; D'Abramo, M.; Orozco, M. Theoretical Characterization of the Dynamical Behavior and Transport Properties of α,γ-Peptide Nanotubes in Solution. *J. Am. Chem. Soc.* **2009**, *131*, 15678−15686.

(3) Liu, J.; Fan, J. F.; Tang, M.; Cen, M.; Yan, J. F.; Liu, Z.; Zhou, W. Q. Water Diffusion Behaviors and Transportation Properties in Transmembrane Cyclic hexa-, octa- and deca-Peptide Nanotubes. *J. Phys. Chem. B* **2010**, *114*, 12183−12192.

(4) Rahmat, F.; Thamwattana, N.; Cox, B. J. Modelling Peptide Nanotubes for Artificial Ion Channels. *Nanotechnology* **2011**, *22*, No. 445707.

(5) Mamonov, A. B.; Kurnikova, M. G.; Coalson, R. D. Diffusion Constant of K^+ inside Gramicidin A: A Comparative Study of Four Computational Methods. *Biophys. Chem.* **2006**, *124*, 268−278.

(6) Baştuğ, T.; Chen, P. C.; Patra, S. M.; Kuyucak, S. Potential of Mean Force Calculations of Ligand Binding to Ion Channels from Jarzynski's Equality and Umbrella Sampling. *J. Chem. Phys.* **2008**, *128*, No. 155104.

(7) Li, Y.; Andersen, O. S.; Roux, B. Energetics of Double-ion Occupancy in the Gramicidin A Channel. *J. Phys. Chem. B* **2010**, *114*, 13881−13888.

(8) Liu, D. Y.; Fan, J. F.; Song, X. Z.; Li, R.; Li, H. MD Simulations on the Influences of an External Force on the Water Transportation Behavior through a Cyclic Peptide Nanotube. *Comput. Mater. Sci.* **2013**, *78*, 47−54.

(9) Liu, J.; Fan, J. F.; Cen, M.; Song, X. Z.; Liu, D. Y.; Zhou, W. Q.; Liu, Z.; Yan, J. F. Dependences of Water Permeation through Cyclic octa-Peptide Nanotubes on Channel Length and Membrane Thickness. *J. Chem. Inf. Model.* **2012**, *52*, 2132−2138.

(10) Li, H.; Fan, J. F.; Li, R.; Yu, Y.; Yan, X. L. Molecular Dynamics Studies on the Influences of a Gradient Electric Field on the Water Chain in a Peptide Nanotube. *J. Mol. Model.* **2014**, *20*, 1−11.

(11) Bucher, D.; Guidoni, L.; Carloni, P.; Rothlisberger, U. Coordination Numbers of K^+ and Na^+ Ions inside the Selectivity Filter of the KcsA Potassium Channel: Insights from First Principles Molecular Dynamics. *Biophys. J.* **2010**, *98*, L47−L49.

(12) Egwolf, B.; Roux, B. Ion Selectivity of the KcsA Channel: A Perspective from Multi-ion Free Energy Landscapes. *J. Mol. Biol.* **2010**, *401*, 831−842.

(13) Roux, B.; Bernèche, S.; Egwolf, B.; Lev, B.; Noskov, B. Y.; Rowley, C. N.; Yu, H. Ion Selectivity in Channels and Transporters. *J. Gen. Physiol.* **2011**, *137*, 415−426.

(14) Ke, S.; Zangerl, E. M.; Stary-Weinzinger, A. Distinct Interactions of Na^+ and Ca^{2+} Ions with the Selectivity Filter of the Bacterial Sodium Channel NaVAb. *Biochem. Biophy. Res. Commun.* **2013**, *430*, 1272−1276.

(15) Furini, S.; Domene, C. On Conduction in a Bacterial Sodium Channel. *PLoS Comput. Biol.* **2012**, *8*, No. e1002476.

(16) Corry, B.; Thomas, M. Mechanism of Ion Permeation and Selectivity in a Voltage Gated Sodium Channel. *J. Am. Chem. Soc.* **2012**, *134*, 1840−1846.

(17) He, Z. J.; Zhou, J.; Lu, X. H.; Corry, B. Ice-like Water Structure in Carbon Nanotube (8,8) Induces Cationic Hydration Enhancement. *J. Phys. Chem. C* **2013**, *117*, 11412−11420.
(18) García-Fandiño, R.; Sansom, M. S. P. Designing Biomimetic Pores Based on Carbon Nanotubes. *Proc. Natl. Acad. Sci. U.S.A* **2012**, *109*, 6939−6944.
(19) Shao, Q.; Zhou, J.; Lu, L. H.; Lu, X. H.; Zhu, Y. D.; Jiang, S. Y. Anomalous Hydration Shell Order of Na^+ and K^+ inside Carbon Nanotubes. *Nano Lett.* **2009**, *9*, 989−994.
(20) Sumikama, T.; Saito, S.; Ohmine, I. Mechanism of Ion Permeation in a Model Channel: Free Energy Surface and Dynamics of K^+ Ion Transport in an Anion-doped Carbon Nanotube. *J. Phys. Chem. B* **2006**, *110*, 20671−20677.
(21) Song, C.; Corry, B. Intrinsic Ion Selectivity of Narrow Hydrophobic Pores. *J. Phys. Chem. B* **2009**, *113*, 7642−7649.
(22) Ghadiri, M. R.; Granja, J. R. Artificial Transmembrane Ion Channels from Self-assembling. *Nature* **1994**, *369*, 301−304.
(23) Hwang, H.; Schatz, G. C.; Ratner, M. A. Steered Molecular Dynamics Studies of the Potential of Mean Force of a Na^+ or K^+ Ion in a Cyclic Peptide Nanotube. *J. Phys. Chem. B* **2006**, *110*, 26448−26460.
(24) Sumiya, N.; Igami, D.; Takeda, K. Molecular Dynamical Study on Ion Channeling through Peptide Nanotube. *AIP Conf. Proc.* **2011**, *1399*, 1055−1056.
(25) Choi, K. M.; Kwon, C. H.; Kim, H. L.; Hwang, H. Potential of Mean Force Calculations for Ion Selectivity in a Cyclic Peptide Nanotube. *Bull. Korean Chem. Soc.* **2012**, *33*, 911−916.
(26) Song, X. Z.; Fan, J. F.; Liu, D. Y.; Li, H.; Li, R. Molecular Dynamics Study of Na^+ Transportation in a Cyclic Peptide Nanotube and Its Influences on Water Behaviors in the Tube. *J. Mol. Model.* **2013**, *19*, 4271−4282.
(27) García-Fandiño, R.; Amorín, M.; Castedo, M.; Granja, J. R. Transmembrane Ion Transport by Self-assembling α, γ-Peptide Nanotubes. *Chem. Sci.* **2012**, *3*, 3280−3285.
(28) Asthagiri, D.; Bashford, D. Continuum and Atomistic Modeling of Ion Partitioning into a Peptide Nanotube. *Biophys. J.* **2002**, *82*, 1176−1189.
(29) Dehez, F.; Tarek, M.; Chipot, C. Energetics of Ion Transport in a Peptide Nanotube. *J. Phys. Chem. B* **2007**, *111*, 10633−10635.
(30) Carvajal-Diaz, J. A. Electrophoretic Transport of Na^+ and K^+ Ions within Cyclic Peptide Nanotube. *Theoretical Investigation of Self-assembled Peptide Nanostructures for Biotechnological and Biomedical Applications*; Texas A&M University: College Station, TX, 2011.
(31) Shao, Q.; Huang, L. L.; Zhou, J.; Lu, L. H.; Zhang, L. Z.; Lu, X. H.; Jiang, S. Y.; Gubbins, K.; Shen, W. F. Molecular Simulation Study of Temperature Effect on Ionic Hydration in Carbon Nanotubes. *Phys. Chem. Chem. Phys.* **2008**, *10*, 1896−1906.
(32) Wanprakhon, S.; Tongraar, A.; Kerdcharoen, T. Hydration Structure and Dynamics of K^+ and Ca^{2+} in Aqueous Solution: Comparison of Conventional QM/MM and ONIOM-XS MD Simulations. *Chem. Phys. Lett.* **2011**, *517*, 171−175.
(33) Rowley, C. N.; Roux, B. The Solvation Structure of Na^+ and K^+ in Liquid Water Determined from High Level ab Initio Molecular Dynamics Simulations. *J. Chem. Theory Comput.* **2012**, *8*, 3526−3535.
(34) Vukovic, L.; Vokac, E.; Král, P. Electroosmotic Phenomena in Thin Neutral Nanotubes. *J. Phys. Chem. Lett.* **2014**, *5*, 2131−2137.
(35) Liu, J.; Fan, J. F.; Tang, M.; Zhou, W. Q. Molecular Dynamics Simulation for the Structure of the Water Chain in a Transmembrane Peptide Nanotube. *J. Phys. Chem. A* **2010**, *114*, 2376−2383.
(36) Humphrey, W.; Dalke, A.; Schulten, K. VMD: Visual Molecular Dynamics. *J. Mol. Graphics* **1996**, *14*, 33−38.
(37) Phillips, J. C.; Braun, R.; Wang, W.; Gumbart, J.; Tajkhorshid, E.; Villa, E.; Chipot, C.; Skeel, R. D.; Kale, L.; Schulten, K. Scalable Molecular Dynamics with NAMD. *J. Comput. Chem.* **2005**, *26*, 1781−1802.
(38) Brooks, B. R.; Bruccoleri, R. E.; Olafson, B. D.; States, D. J.; Swaminathan, S.; Karplus, M. CHARMM: A Program for Macromolecular Energy, Minimization and Dynamics Calculations. *J. Comput. Chem.* **1983**, *4*, 187−217.
(39) Jorgensen, W. L.; Chandrasekhar, J.; Madura, J. D.; Impey, R. W.; Klein, M. L. Comparison of Simple Potential Functions for Simulating Liquid Water. *J. Chem. Phys.* **1983**, *79*, 926−935.
(40) Darden, T. A.; York, D. M.; Pedersen, L. G. Particle Mesh Ewald: An N-log (N) Method for Ewald Sums in Large Systems. *J. Chem. Phys.* **1993**, *98*, 10089.
(41) Martyna, G. J.; Tobias, D. J.; Klein, M. L. Constant Pressure Molecular Dynamics Algorithms. *J. Chem. Phys.* **1994**, *101*, 4177−4189.
(42) Ryckaert, J. P.; Ciccotti, G.; Berendsen, H. J. Numerical Integration of the Cartesian Equations of Motion of a System with Constraints: Molecular Dynamics of *n*-Alkanes. *J. Comput. Phys.* **1977**, *23*, 327−341.
(43) Darve, E.; Pohorille, A. Calculating Free Energies Using Average Force. *J. Chem. Phys.* **2001**, *115*, 9169−9183.
(44) Darve, E.; Rodríguez-Gómez, D.; Pohorille, A. Adaptive Biasing Force Method for Scalar and Vector Free Energy Calculations. *J. Chem. Phys.* **2008**, *128*, No. 144120.
(45) Li, R.; Fan, J. F.; Li, H.; Yan, X. L.; Yu, Y. Exploring the Dynamic Behaviors and Transport Properties of Gas Molecules in a Transmembrane Cyclic Peptide Nanotube. *J. Phys. Chem. B* **2013**, *117*, 14916−14927.
(46) Liu, H. F.; Chen, J.; Shen, Q.; Fu, W.; Wu, W. Molecular Insights on the Cyclic Peptide Nanotube-mediated Transportation of Antitumor Drug 5-Fluorouracil. *Mol. Pharmaceut.* **2010**, *7*, 1985−1994.
(47) Vijayaraj, R.; Van Damme, S.; Bultinck, P.; Subramanian, V. Theoretical Studies on the Transport Mechanism of 5-Fluorouracil through Cyclic Peptide Based Nanotubes. *Phys. Chem. Chem. Phys.* **2013**, *15*, 1260−1270.
(48) Smith, G. R.; Sansom, M. S. P. Effective Diffusion Coefficients of K^+ and Cl^- Ions in Ion Channel Models. *Biophys. Chem.* **1999**, *79*, 129−151.
(49) Zhou, J.; Lu, X. H.; Wang, Y. R.; Shi, J. Molecular Dynamics Study on Ionic Hydration. *Fluid. Phase. Equilibr.* **2002**, *194*, 257−270.
(50) Zimmerli, U.; Gonnet, P. G.; Walther, J. H.; Koumoutsakos, P. Curvature Induced L-Defects in Water Conduction in Carbon Nanotubes. *Nano Lett.* **2005**, *5*, 1017−1022.

DOI: 10.1021/acs.jcim.5b00025
J. Chem. Inf. Model. 2015, 55, 998−1011